

THE PROVENANCE OF HIGH-TITANIUM CUMULATE 71597. P. H. Donohue*¹ and C. R. Neal¹, ¹Civil & Environmental Engineering & Earth Sciences, University of Notre Dame, Notre Dame, IN (*pdonohu1@nd.edu).

Introduction: There are seven known lunar olivine cumulate basalts: Apollo 12 basalts 12005 and 12036 [1-2], Apollo 15 basalts 15385 and 15387 [3], Apollo 14 clast 14305,122 [4], Apollo 17 basalt 71597 [5-6], and six fragments in lunar meteorite NWA773 [7]. Of these, the only high-titanium cumulate is sample 71597, which has 8.4 wt.% TiO₂ [5]. Whole-rock analyses (major and trace element) and mineral compositions (major element) indicated basalt 71597 experienced 24-27% olivine and possible minor ilmenite accumulation [6].

Aspects of mare volcanic processes and the nature of olivine accumulation (*e.g.*, gravitational settling during a single, large flow *vs.* magma mixing) can be addressed by quantitative petrography (*via* crystal size distributions) and mineral geochemistry (*via* crystal stratigraphy). We present electron probe microanalysis (EPMA) and laser ablation inductively couple plasma mass spectrometry (LA-ICP-MS) analyses of mineral phases in two thin sections of basalt 71597 (,12 and ,13). Microscale details of basalt evolution are recorded in core-to-rim and inter-crystal compositional variations, and can best be constrained by *in-situ* techniques. Cumulate 71597 is of particular interest because it is a textural and compositional end-member of the high-Ti basalts. In addition, equilibrium liquid trace element compositions are used to constrain a petrogenetic model of magma evolution.

Textural Analysis: Crystal size distributions (CSDs) for olivine, ilmenite, pyroxene, and plagioclase in 71597 have been previously presented [8]. CSD profiles [8] can be used to calculate residence times of crystals by assuming growth rates (*cf.*, [9]). Growth rates are time and temperature dependent, and the coarse groundmass indicates a slow cooling rate. Thus the average of the three longest high-T runs (960°C/360 hr, 970°C/596 hr, and 990°C/224 hr) from [10] are used to obtain growth rates for pyroxene (2.91×10^{-10} cm s⁻¹), plagioclase (2.49×10^{-10} cm s⁻¹), and ilmenite (1.35×10^{-10} cm s⁻¹). Olivine residence times are calculated using the average growth rates reported in [11] of 1.5×10^{-11} cm s⁻¹.

Mineral Chemistry Analytical Methods: Major element compositions of select ilmenite, pyroxene, plagioclase and olivine crystals were obtained using a JEOL JXA-8200 EMP at the Earth and Planetary Sciences Microanalysis Facility, Washington University in St. Louis (St. Louis, MO). The EMP was equipped with five wavelength-dispersive spectrometers and a JEOL (e2v/Gresham) silicon-drift energy-dispersive

spectrometer. Typical operating conditions were 15 KV accelerating potential and 25 nA probe current and a 5 micrometer spot size. A defocused beam (typically ~10 micrometers diameter) was used to avoid loss of volatiles (*e.g.*, Na, K) during plagioclase analyses.

Compositional analyses of several large (>10 μm) melt inclusions in olivine and ilmenite crystals, as well as additional olivine (spot and line raster), armalcolite, and mesostasis analyses were obtained using a Cameca SX50 EMP at the University of Chicago (Chicago, IL). Line raster analyses were obtained across two large, partially resorbed olivines in 71597,12. Typical operating conditions were 15 KV accelerating potential and a 30 nA probe current and a 1 or 5 micrometer spot size (for oxides and silicates, respectively).

Trace element abundances for a subset of EPMA crystals were obtained using an Element2 ICP-MS coupled to a UP213 Nd:YAG laser ablation system at the Notre Dame Midwest Isotope and Trace Element Research Analytical Center (MITERAC, Notre Dame, IN). The EPMA were utilized as internal standards. Data were reduced using the GLITTER[®] software [12], which allows for time-resolved background (~50 seconds) and signal (~60 seconds) selection. Cracks, inclusions and adjacent phases were avoided using a combination of transmitted and reflected light prior to ablation and confirmed by time-resolved signal review. Equilibrium liquids were calculated from mineral compositions using literature partition coefficients of [13].

Crystallization of 71597: The trace element variations imply a heterogeneous distribution of trace elements and/or that olivine accumulated from different magma packets. This could be from different areas within a thick flow or from different batches of magma that erupted through the same vent system so these olivines would have been effectively ripped from the conduit walls by the 71597 parent magma. Olivine crystallized first at an initial cooling rate of 1-3°C/hr. Large olivine phenocrysts CSD profiles [8] yield residence times of ~12 years. A smaller olivine size population (<0.3mm) co-crystallized with ilmenite as these phases have similar residence times of 1.4-1.6 years. Groundmass plagioclase, pyroxene, and ilmenite indicate post-emplacement cooling over 0.2-0.5 years. The variation in modal olivine between our analysis (sections ,12 and ,13) and that of 71597 (two unreported subsample numbers [6]) indicates heterogeneities in the accumulation of olivine at the thin section scale. Olivine was on the liquidus prior to eruption, and some

matrix olivines likely crystallized at the surface. The residence times of the larger size population of ilmenite and matrix olivine are similar (1.4-1.6 years), and these early phases crystallized together post-eruption.

Ilmenite contains relatively high MgO contents (3.2-5.2 wt.% MgO here, up to 8 wt.% noted by [6]) compared to other Apollo 17 high-Ti basalts (0.17-4.87 wt.% MgO), which may have resulted from subsolidus reaction with the high-Mg melt during slow cooling. This is supported by abundant exsolution lamellae similar to those found in other re-equilibrated ilmenite from coarse-grained Apollo 17 basalts [14]. This high Mg is likely promoted by some olivine resorption, with titanite and high-Ca plagioclase crystallization lowering CaO leading to pigeonite crystallization. Fig. 1a demonstrates the crystallization path of olivine crystallization lowering Cr, followed by resorption, possibly as olivine clasts are ripped up by new magma, which buffers Cr during augite crystallization. Subsequent crystallization of augite and additional olivine again lowers the magma Cr content. There may also be a contribution from diffusion, which could produce the lack of Fe-enrichment observed during pyroxene crystallization [1]. Titanite is present as discrete crystals and as mantles (up to 0.3 mm) on olivine, while

pigeonite is limited to extreme margins of augite and small crystals near the margins of partially resorbed olivine.

Type Source of 71597: Apollo 17 high-Ti basalts are separated into 5 groups (Types A, B1, B2, C, D) on the basis of whole-rock major and trace element chemistry [13]. For example, the Type B basalt suite first identified by [15] and later split into Types B1 and B2 were divided on the basis of REE and HFS abundance and La/Sm ratios [13]. Prior to the split, [16] proposed 71597 originated in a high-Ti basalt flow of Apollo 17 Type B basalt composition. On Fig. 1b, the whole-rock fractionation trends of La and Eu in Apollo 17 high-Ti basalts are compared to the plagioclase and pyroxene equilibrium liquids (phases for which there are La and Eu data). Pigeonite equilibrium compositions, as expected, do not appear to represent true liquid compositions. Finally, relatively late-stage plagioclase crystallization follows the fractionation trend from a 71597 whole-rock starting composition. Augite is consistent with derivation from a Type B2 basalt parental magma.

We have presented here the case for placing a previously unclassified basalt into an existing chemical suite using crystal stratigraphy. Approximately one-third of high-Ti mare basalts returned by the Apollo 17 mission are currently classified as Type U basalts. As a result of this work, we suggest the crystal stratigraphy method has demonstrated potential for classifying these basalts.

References: [1] Dungan M. A. and Brown R. W. (1977) *Proc. Lunar Sci. Conf. 8th*, 1339–1381. [2] Rhodes J. M. *et al.* (1977) *Proc. Lunar Sci. Conf. 8th*, 1305–1338. [3] Ryder G. (1985) *Curatorial Branch Publication* 72, 1–443. [4] Taylor L. A. *et al.* (1983) *Earth Planet. Sci. Lett.* 66, 33–47. [5] Murali A. V. *et al.* (1977) *Lunar Planet. Sci. Conf. VIII*, 703–704. [6] Warner R. D. *et al.* (1977) *Proc. Lunar Sci. Conf. 8th*, 1429–1442. [7] Jolliff B. L. *et al.* (2003) *Geochim. Cosmochim. Acta* 67, 4857–4879. [8] Donohue P. H. and Neal C. R. (2012) *Lunar Planet. Sci. Conf. 44*, Abs #2077. [9] Marsh B. (1988) *Contrib. Mineral. Petrol.* 99, 277–291. [10] Burkhard D. J. M. (2005) *Eur. J. Mineral.* 17, 675–686. [11] Vinet N. and Higgins M. D. (2010) *J. Petrol.* 51, 1297–1332. [12] van Achterbergh E. *et al.* (2001) Mineral. Ass. Canada, Short Course 40, 239–243. [13] Neal C. R. *et al.* (1990) *Geochim. Cosmochim. Acta* 54, 1817–1833. [14] El Goresy A. and Ramdohr P. (1975) *Proc. Lunar Sci. Conf. 6th*, 729–745. [15] Rhodes J. M. *et al.* (1976) *Proc. Lunar Sci. Conf. 7th*, 1467–1489. [16] Warner R. D. *et al.* (1979) *Proc. Lunar Planet. Sci. Conf. 10th*, 225–247.

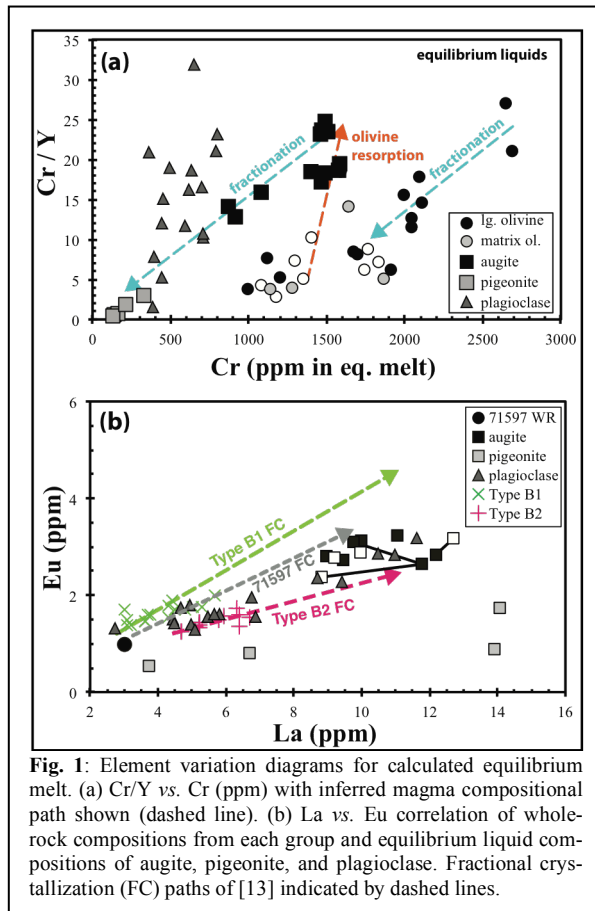


Fig. 1: Element variation diagrams for calculated equilibrium melt. (a) Cr/Y vs. Cr (ppm) with inferred magma compositional path shown (dashed line). (b) La vs. Eu correlation of whole-rock compositions from each group and equilibrium liquid compositions of augite, pigeonite, and plagioclase. Fractional crystallization (FC) paths of [13] indicated by dashed lines.